Non-Negligible Influences of Rain on 5G Millimeter Wave Terrestrial Communication System

Abstract: The impacts of rain on millimeter wave (mmW) terrestrial links, which are inevitably affected by ground-objects-induced multipath propagation, are presented based on the signal time series data measured at 35 GHz. We analyze the coupled influence mechanism of rain-induced and ground-objects-induced multipath propagation on mmW terrestrial links. It can be deduced that the rain-induced impacts on millimeter wave terrestrial links cannot be neglected. The results given in this paper are significant for developing 5G millimeter wave terrestrial mobile communication links.

Keywords: 5G communication; mmW; multipath; rain-caused effects; terrestrial links

GONG Shuhong[1], ZHANG Xingmin[1], DOU Jianwu[2], HUANG Weifang[2]

(1. School of Physics and Optoelectronic Engineering, Xidian University, Xi'an 710071, China;
2. Algorithm Department, ZTE Corporation, Shanghai 200240, China)

DOI: 10.12142/ZTECOM.202003010

http://kns.cnki.net/kcms/detail/34.1294.TN.20200317.1006.003.html, published online March 17, 2020

Manuscript received: 2019-01-15

Citation (IEEE Format): S. H. Gong, X. M. Zhang, J. W. Dou, et al., "Non-negligible influences of rain on 5G millimeter wave terrestrial communication system," *ZTE Communications*, vol. 18, no. 3, pp. 64 – 70, Sept. 2020. DOI: 10.12142/ZTECOM.202003010.

1 Introduction

Millimeter wave (mmW) technology is regarded as a key technology for 5G mobile communication system, because it is greatly helpful for solving the bottleneck problems, which are the main contradictions between the required traffic in the future and the current 2G, 3G and 4G communication systems[1 – 5]. Meanwhile, it is also necessary to face more complex propagation characteristics for fully taking advantage of millimeter wave technology[6 – 8].

One of the principal technical difficulties for mmW technology is to evaluate the impacts of the troposphere, such as rain-induced attenuation, depolarization and noise. The propagation characteristics of millimeter wave in the troposphere have been regarded as an important part of radio wave propagation field[9]. Many calculating models and measured data about the propagation properties are given, and ITU-R models may be the most authoritative and reliable[10 – 11]. In general, rain-induced impacts are the most severe impacts and the first aspect to consider. Therefore, rain-induced impacts are also presented in 5G plans. Some publications[12 – 15] think that the rain-induced impacts on the terrestrial cellular scale link with several hundred meters of path length do not cause significant additional influences and even can be ignored, which is concluded based on the calculating results using the ITU-R models.

However, 5G mobile communication system will be applied to complex terrain and ground objects environment[7 – 8]. Consequently, the multipath propagation caused by terrain or ground objects is inevitable. Recent studies have revealed that the multipath propagation is an important factor affecting the millimeter-wave propagation characteristics[9 – 10]. Hence, with the increasing complexity of terrain and ground objects, the multipath effect is a key factor to affect the propagation characteristics of radio waves in 5G ground mobile link[16].

When it rains, multipath signals caused by terrain or ground objects will interact with raindrop particles, which may lead to more complex multipath signals[17 – 19]. In other words, every path will be affected by raindrop-caused random absorption and scattering, so the multipath signal is randomly changing. As a result, received signals include the multipath signals caused by raindrops scattering and/or by terrain or ground objects. A possible special case is that the raindrop absorption effect may also remove some terrain or ground objects-caused direct wave signals from the received signals, which means that those terrain or ground objects-caused signal arrival direc-

This work was supported in part by ZTE Corporation Program under Grant No. 2017ZTE01-01-06.

tions are objectively exist but the signals from those directions just contain the multipath signals caused by raindrop scattering. In a word, when a rain event occurs, the received signals in a complex terrain and ground object environment are likely to include two different kinds of multipath signals. According to the theory of vector superposition, the two different multipath signals will couple together and finally modulate channel effects together. The two kinds of multipath signals may cause destructive or constructive interference and magnify the atmospheric transmission effects. Namely, the integrated impacts caused by rain are likely to be much more serious than the effects forecasted by the ITU-R models, which are suitable for the propagation situation free from the effects of terrain and ground objects. Therefore, it may not be reliable to determine if the rain-induced effects can be ignored just according to the calculation results with the ITU-R models, and it is necessary to estimate the impacts of rain on mmW terrestrial links.

In this paper, the receiving signal time series at 35 GHz are measured in a selected multipath environment. The equivalent attenuation is obtained by comparing the received signals in rain with those measured in clear air. The measured data imply that, under a certain rain rate condition, the measured equivalent attenuation is much greater than the rain-induced attenuation calculated by the ITU-R P.530-12 model. The reasons for the enormous difference are analyzed by theoretical and experimental methods. According to the analysis results, it can be concluded that the transmission effects on mmW terrestrial links, such as attenuation-induced fade, equivalent attenuation, phase-shift, and atmosphere noise, in rain environment cannot be estimated by the classical models, which are built for computing the impacts induced solely by rain on mmW line of sight (LOS) links. In other words, it is necessary to adopt a completely new method for evaluating the transmission effects on mmW terrestrial links in a rain environment, such as fading, depolarization, noise, and phase shift. The conclusions given in this paper are significant for developing 5G mmW terrestrial links.

2 Equivalent Attenuation Measured in Selected Multipath Environment Under Rain Condition

Rain-induced attenuation should be the first consideration for designing mmW terrestrial links that work in a multipath environment. In order to study rain-induced attenuation characteristics of such the mmW links, we conducted a testing experiment using a terrestrial link at 35 GHz. The testing experiment system includes two parts: meteorological parameter measurement system and equivalent attenuation measurement system. As shown in **Fig. 1a**, the meteorological parameter measurement system is composed of an OTT Parsivel laser particle spectrometer and a computer. The equivalent attenuation measurement system includes a transmitter, a receiver, a spectrum analyzer and a computer, which are shown in **Fig. 1b**. The technical parameters of the OTT Parsivel laser particle spectrometer can be found in any official specification, which will not be introduced in this paper. The main parameters of the transmitter and the receiver are listed in **Table 1**.

In order to investigate the influence of rain on mmW terrestrial links, the testing system was located at the 5th floor of the West Building of Xidian University, where the random-ground-objects-induced multipath propagation can be neglected with very high approximation, but the static-ground-objects-induced multipath propagation was taken into consideration. **Fig. 2** shows the testing scenario, where the receiving and transmitting antennas are on the same side, namely, the receiving antenna can receive the signals reflected from the ground and the opposite wall. It should be noted that the Fresnel main region cannot be used to estimate the occurrence or nonoccurrence of multipath propagation, because it is only valid for the incidence case of a plane wave from a transmitting antenna to a receiving antenna. It is obvious that the propagation scenario in Fig. 2 is not the plane wave incidence case.

Fig. 3 shows our testing flow, where a spectrum analyzer is connected with the output port of the receiver's downconverter, hence the spectrum analyzer monitors the power level of re-

(a) Meteorological parameter measurement system (b) Equivalent attenuation measurement system

▲ **Figure 1. Testing experiment system of meteorological parameter measurement.**

▼**Table 1. Main parameters of the transmitter and the receiver**

(a) Parameters of the transmitting antenna and the receiving antenn

Polarization	Circular Honor Diameter	Half Power Beam Width of E Plane or H Plane	Gain
Right-handed circular polarization	50 mm	6°	17 dB

(b) Parameters of the transmitter

Output Frequency	Bandwidth	Output Power
35 GHz	<100 MHz	10 dBm±0.1 dBm

(c) Parameters of the receiver

Thresholds Power	Power Resolution	Output Frequency from Downconverter
−105 dBm	0.1 dBm	1.2 GHz

ceived signals and saves them into the computer by every minute; at the same time, the atmospheric parameters are recorded. The rain-induced equivalent attenuation time sequence can be obtained by subtracting the power level time sequence in rain from the reference power level. Note that the reference power level is the average power level of the signals that are received within 20 minutes before every rain event occurs.

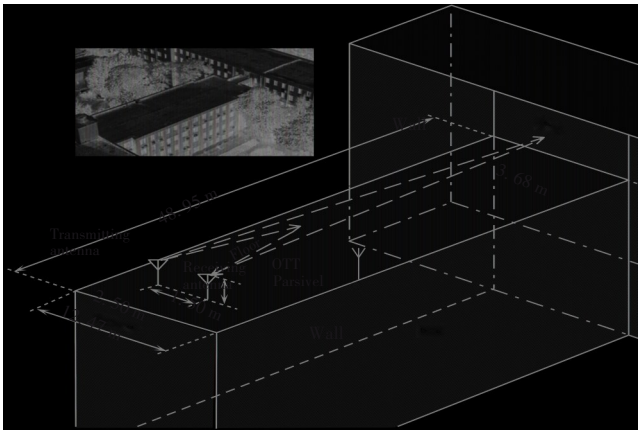

▲**Figure 2. Testing scenario in static-ground-objects-induced multipath propagation environment.**

During the measurement period from August 2017 to January 2018, about 3 500 minute time sequence of one-minute integration rain rate and the corresponding equivalent attenuation time series were recorded. In order to investigate the rain-induced influence on mmW terrestrial links, the rain-induced attenuation of 100 m path for the measured rain rate data is calculated by

$$A_{\text{calculation}} = (a_r R^{b_r}) \cdot 0.1, \tag{1}$$

$$a_r = \frac{1}{2}(a_h + a_v), \tag{2}$$

$$b_r = \frac{1}{2a_r}(a_h b_h + a_v b_v). \tag{3}$$

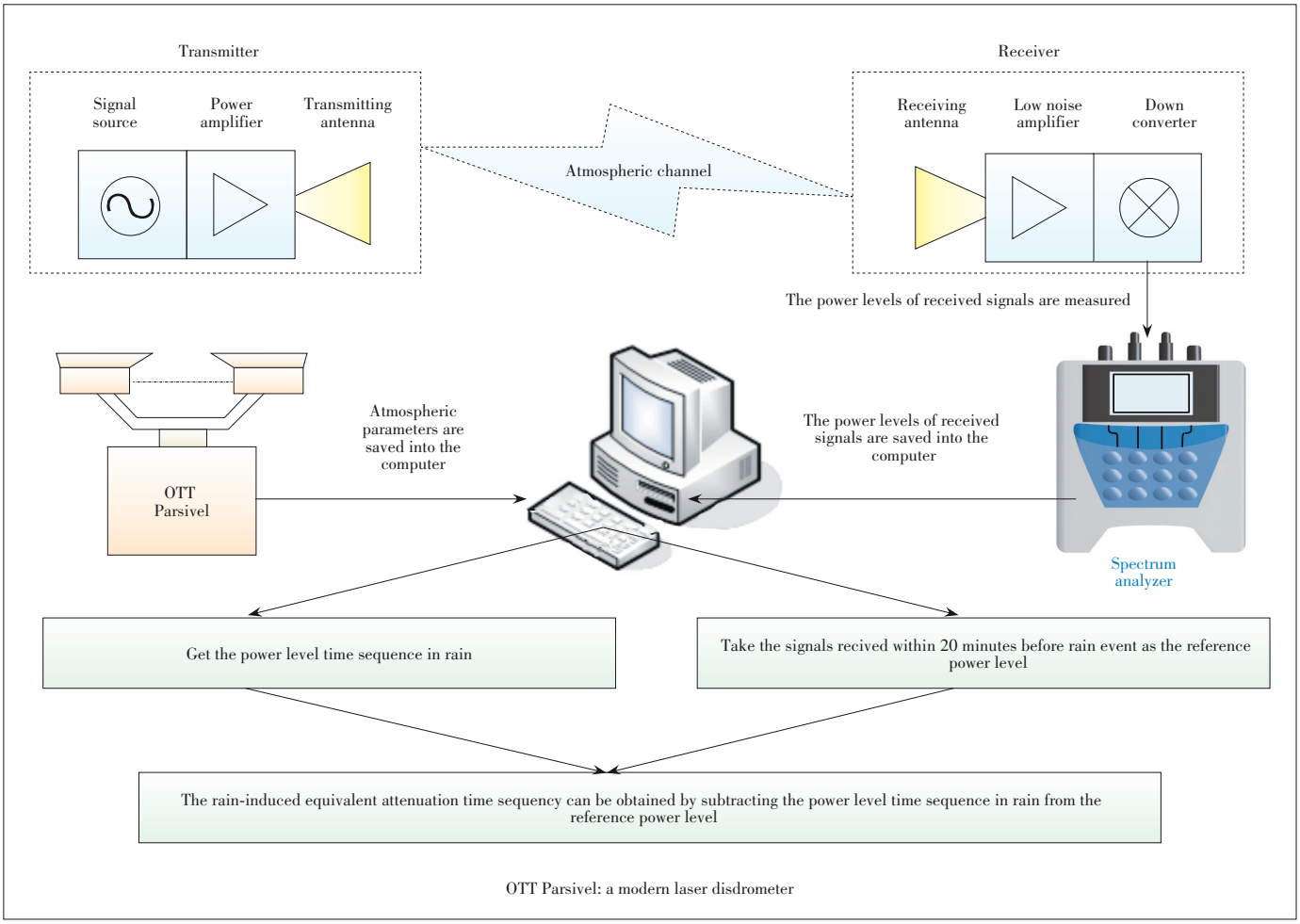

▲**Figure 3. Testing flow chart of meteorological parameter measurement.**

R in Eq. (1) notes the one-minute integration rain rate, which is replaced by the measured rain rate given in **Fig. 4**. a_h, a_v, b_h and b_v in Eqs. (2) and (3) are taken as a_h = 0.3374, a_v = 0.3224, b_h = 0.9047 and b_v = 0.8761 at 35 GHz, which are given in ITU-R P.838-3. Eq. (1) implies that it is true that the rain rate along the 100 m path in Fig. 2 is the same as that at the testing position. The measured equivalent attenuation and the calculated attenuation are shown in Fig. 4.

It is obvious that the values of the measured equivalent attenuation testing are larger than those of the calculated attenuation. The difference may be caused by the fact that the rain-induced attenuation is dependent not only on the rainfall type, raindrops' shape and size distribution, which determine the coefficients of a_h, a_v, b_h and b_v in Eqs. (2) and (3), but also on the space distribution of the rain rate, which determines the equivalent path length. In other words, the difference may arises from wrong values of a_h, a_v, b_h and b_v or the unseemly approximation of taking the geometry path length 0.1 km as the equivalent path length in Eq. (1). In addition, the difference in Fig. 4 may also be generated by wet antenna[20 – 23]. In order to verify the guesses mentioned above, another measurement in non-multipath environment was carried out. **Fig. 5** shows the testing scenario, which is the north campus of Xidian University. The transmitter and the receiver were placed on the top of two buildings with a distance of 820 m, respectively, and the height difference between the transmitter and the receiver was about 20 m. It was sure that there were no ground objects in the Fresnel region of the link in Fig. 5, the radius of which was about $0.5\sqrt{820 \times 0.0086}$ = 1.3256 m. In addition, it was sure that there were no ground objects in the two antennas' common beam space. Therefore, it is logical to consider the link in Fig. 5 as a LOS link.

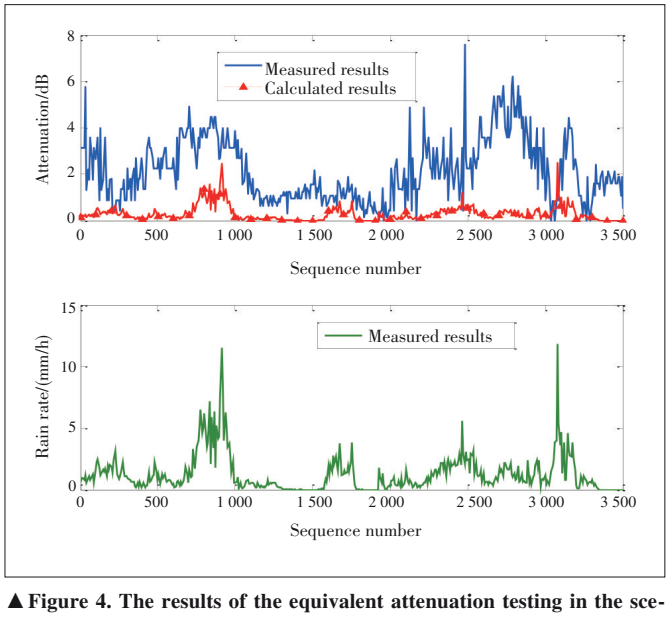

▲**Figure 4. The results of the equivalent attenuation testing in the scenario given in Figure 2.**

▲**Figure 5. Test scenario in line of sight (LOS) propagation environment.**

During the measurement period from March 2018 to June 2018, about 12 000 min time sequence of one-minute integration rain rate and the corresponding equivalent attenuation time series were recorded. The rain-induced attenuation was also calculated by Eq. (1). The measured attenuation and the calculated attenuation are shown in **Fig. 6**.

Fig. 6 shows that the measured attenuation and the calculated attenuation are approximatively matched. The subtle difference should be caused by the wet antenna mentioned in Refs. [20] – [23]. The results in Fig. 6 verify that the difference between the measured data and the calculated data in Fig. 4 is not mainly caused by the wrong a_h, a_v, b_h and b_v or the unseemly approximation of taking the geometry path length 0.1 km as the equivalent path length in Eq. (1). In other words, the obvious difference in Fig. 4 is likely to be caused by the coupled influence of rain-caused effects and ground-objects-induced multipath propagation, and it is not reasonable to regard rain-induced attenuation and other impacts on mmW terrestrial links as negligible factors just according to the traditional models, which are used to estimate the effects caused individually by rain. In what follows, the coupled influence mechanism of rain-caused effects and ground-objects-induced multipath propagation on mmW terrestrial link will be qualitatively analyzed.

3 Coupled Influence Mechanism of Rain-Caused Effects and Ground-Objects-Induced Multipath Propagation on MmW Terrestrial Links

In fact, the random variation of the power level received in the measured environment in Fig. 5 is attenuation-induced fade, and the attenuation is caused individually by rain. Furthermore, Eq. (1) is just used to calculate the attenuation induced solely by rain. Consequently, the attenuation calculated by Eq. (1) is approximatively matched with that obtained by subtracting the power level time sequence in rain from the ref-

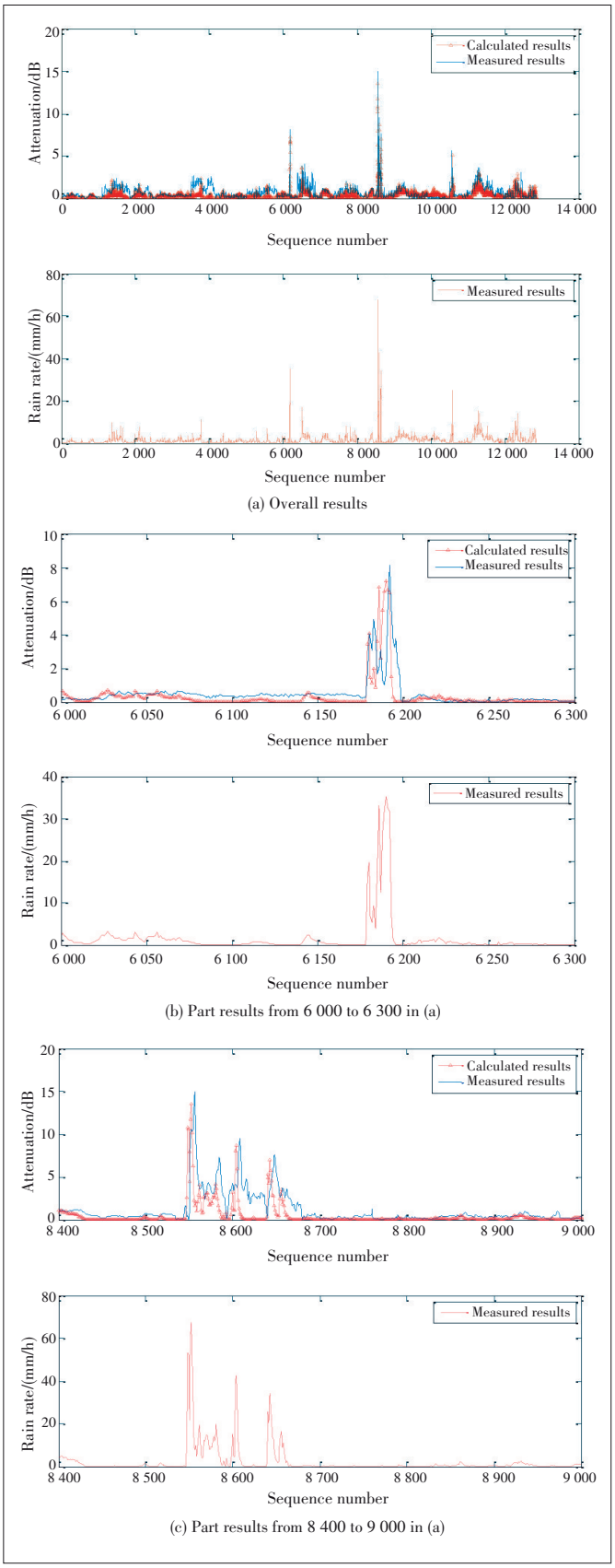

▲Figure 6. Results of attenuation testing in the scenario given in Figure 5.

erence power level, which is simply introduced in Section 2. However, each path of the multipath in Fig. 2 is affected by rain-induced effects, such as attenuation and phase shift. That is, the fade of the power level received in the scenario in Fig. 2 is induced by rain-caused multipath propagation. However, Eq. (1) is just used to calculate the attenuation induced only by rain. Therefore, the obvious difference in Fig. 4 is inevitable and not surprising at all.

In order to qualitatively analyze the coupled influence mechanism of rain-caused effects and ground-objects-induced multipath propagation on mmW terrestrial links, the simplest two-path propagation case is considered (**Fig. 7**). Suppose the vector complex amplitudes at the receiving antenna via Path-1 and Path-2 are $\mathbf{E}_1$ and $\mathbf{E}_2$, respectively. The vector complex amplitude of the total field can be written as

$$\mathbf{E} = \mathbf{E}_1 + \mathbf{E}_2. \tag{4}$$

The module $|\mathbf{E}|$ of $\mathbf{E}$ can be calculated by

$$|\mathbf{E}| = \sqrt{|\mathbf{E}_1|^2 + |\mathbf{E}_2|^2 + 2|\mathbf{E}_1| \cdot |\mathbf{E}_2| \cos(\theta_2 - \theta_1)}, \tag{5}$$

where θ_2 and θ_1 are the phase angles of $\mathbf{E}_1$ and $\mathbf{E}_2$. The phase angle θ of $\mathbf{E}$ can be calculated by

$$\theta = \operatorname{arctg} \frac{|\mathbf{E}_1| \sin(\theta_1) + |\mathbf{E}_2| \sin(\theta_2)}{|\mathbf{E}_1| \cos(\theta_1) + |\mathbf{E}_2| \cos(\theta_2)}. \tag{6}$$

Moreover, the total power is proportional to $|\mathbf{E}|^2$, which is expressed as

$$|\mathbf{E}|^2 = |\mathbf{E}_1|^2 + |\mathbf{E}_2|^2 + 2|\mathbf{E}_1| \cdot |\mathbf{E}_2| \cos(\theta_2 - \theta_1). \tag{7}$$

For the similar scenario in Fig. 2, in which the random-ground-objects-induced multipath propagation can be neglected with very high approximation, if rain does not occur, $|\mathbf{E}_1|$, $|\mathbf{E}_2|$ and θ_1, θ_2, are approximatively constant values.

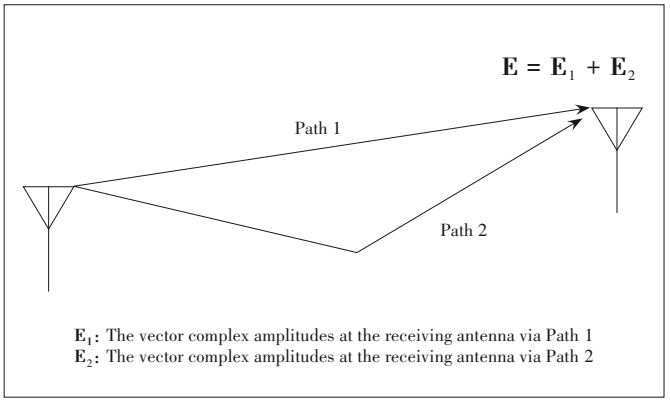

▲Figure 7. The two-path propagation case.

However, once rain occurs, $|\mathbf{E}_1|$, $|\mathbf{E}_2|$ and θ_1, θ_2 become random values because of rain-induced attenuation and scattering. Based on the results in Ref. [24], $|\mathbf{E}_1|$, $|\mathbf{E}_2|$ and θ_1, θ_2 can be expressed as

$$|\mathbf{E}_1| = \langle |\mathbf{E}_1| \rangle + |\mathbf{E}_1|_f, \tag{8}$$

$$|\mathbf{E}_2| = \langle |\mathbf{E}_2| \rangle + |\mathbf{E}_2|_f, \tag{9}$$

$$\theta_1 = \langle \theta_1 \rangle + \theta_{1f}, \tag{10}$$

$$\theta_2 = \langle \theta_2 \rangle + \theta_{2f}, \tag{11}$$

where $\langle |\mathbf{E}_1| \rangle$, $\langle |\mathbf{E}_2| \rangle$ and $\langle \theta_1 \rangle$, $\langle \theta_2 \rangle$ denote the mean values, $|\mathbf{E}_1|_f$, $|\mathbf{E}_2|_f$ and θ_{1f}, θ_{2f} denote the fluctuation induced by random scattering. Rain-induced attenuation and phase-shift determine $\langle |\mathbf{E}_1| \rangle$, $\langle |\mathbf{E}_2| \rangle$ and $\langle \theta_1 \rangle$, $\langle \theta_2 \rangle$, which slowly change. It should be noted that, as mentioned in Section 1, $\langle |\mathbf{E}_1| \rangle$ or $\langle |\mathbf{E}_2| \rangle$ may disappear because of very large attenuation, which means that rain-induced effect removes the terrain or ground objects-caused multipath. Rain-induced scattering determines $|\mathbf{E}_1|_f$, $|\mathbf{E}_2|_f$ and θ_{1f}, θ_{2f}, which rapidly change. $|\mathbf{E}_1|_f$ and $|\mathbf{E}_2|_f$ follow Rice distribution, while θ_{1f} and θ_{2f} follow uniform distribution from 0 to 2π. Therefore, even if in the simplest two-path propagation environment, $|\mathbf{E}|^2$, which is proportional to received power, is expressed as

$$\begin{aligned} |\mathbf{E}|^2 = {} & [\langle |\mathbf{E}_1| \rangle + |\mathbf{E}_1|_f]^2 + [\langle |\mathbf{E}_2| \rangle + |\mathbf{E}_2|_f]^2 + \\ & 2[\langle |\mathbf{E}_1| \rangle + |\mathbf{E}_1|_f] \cdot [\langle |\mathbf{E}_2| \rangle + |\mathbf{E}_2|_f] \cos\Big[(\langle \theta_2 \rangle - \\ & \langle \theta_1 \rangle) + (\theta_{2f} - \theta_{1f}) \Big]. \end{aligned} \tag{12}$$

Based on Eq. (12), it is quite clear that $(|\mathbf{E}_1|_f)^2$, $(|\mathbf{E}_2|_f)^2$ and the complex interference terms of $\langle |\mathbf{E}_1| \rangle \cdot |\mathbf{E}_1|_f$, $\langle |\mathbf{E}_2| \rangle \cdot |\mathbf{E}_2|_f$, $\langle |\mathbf{E}_1| \rangle \cdot \langle |\mathbf{E}_2| \rangle$, $|\mathbf{E}_1|_f \cdot |\mathbf{E}_2|_f$, $|\mathbf{E}_1|_f \cdot \langle |\mathbf{E}_2| \rangle$ and $|\mathbf{E}_2|_f \cdot \langle |\mathbf{E}_1| \rangle$ are introduced into $|\mathbf{E}|^2$. That is, the ground-objects-induced multipath propagation makes rain-induced scattering effect also more complicatedly impact the equivalent attenuation, because the received power is proportional to $|\mathbf{E}|^2$. It can be concluded that $|\mathbf{E}|^2$ will be more complex in more-path propagation environment. Eq. (12) also implies that quantitatively investigating $\langle |\mathbf{E}_1| \rangle$, $\langle |\mathbf{E}_2| \rangle$, $\langle \theta_1 \rangle$, $\langle \theta_2 \rangle$ and $|\mathbf{E}_1|_f$, $|\mathbf{E}_2|_f$, θ_{1f}, θ_{2f} is necessary for quantitatively analyzing $|\mathbf{E}|^2$. However, $\langle |\mathbf{E}_1| \rangle$, $\langle |\mathbf{E}_2| \rangle$, $\langle \theta_1 \rangle$, $\langle \theta_2 \rangle$ and $|\mathbf{E}_1|_f$, $|\mathbf{E}_2|_f$, θ_{1f}, θ_{2f} are decided by not only rain-caused effects but also wet antennas and wet ground surface. The impact of wet antenna on $\langle |\mathbf{E}_1| \rangle$ and $\langle |\mathbf{E}_2| \rangle$ is reported in some publications[20 – 23]. Moreover, it is very complicated to quantitatively analyze $\langle \theta_1 \rangle$, $\langle \theta_2 \rangle$, $|\mathbf{E}_1|_f$, $|\mathbf{E}_2|_f$, and θ_{1f}, θ_{2f} in rainy multipath environments. Therefore, Eq. (12) mathematically analyzes the coupled influence mechanism of rain-caused effects and ground-objects-induced multipath propagation on mmW terrestrial links, but the quantitative analysis of $|\mathbf{E}|^2$ will not be given in this paper. In a word, the traditional model for calculating rain-induced attenuation is suitable for LOS propagation case, while the quantitative analysis of $|\mathbf{E}|^2$ by the model similar to Eq. (12) is necessary for none LOS propagation case in rainy multipath environments. Hence, the obvious difference in Fig. 4 and the approximate accordance in Fig. 6 are logical.

According to the same mechanism, it can be concluded that other rain-induced effects on mmW terrestrial links, such as depolarization, phase-shift and atmosphere noise, cannot be estimated by traditional models, which are used in LOS propagation case. Therefore, the impacts of rain on 5G mmW terrestrial links are likely to be non-negligible on account of the coupled impaction of rain-induced effects and multipath propagation phenomenon, and it is necessary to deeply investigate the impacts of rain on 5G mmW terrestrial links.

4 Conclusions

The transmission effects, such as attenuation-induced fade, equivalent attenuation, phase-shift, and atmosphere noise, on mmW terrestrial links in rain environment are severer than those on mmW LOS links in rain because of the coupled action of rain-induced scattering and ground-objects – induced multipath propagation. For mmW terrestrial links, it is wrong to estimate rain-induced effects using traditional models, such as ITU-R models, which are suitable for LOS propagation cases. In other words, the impacts of rain on 5G mmW terrestrial communication system are likely to be non-negligible on account of the coupled impaction of rain-induced effects and multipath propagation phenomenon. It is necessary to build a model for quantitatively estimating the transmission effects on mmW terrestrial links in rain environment, which has not been included in any previous publications, but the mathematically analytic process in Section 3 is a good start and helpful to build such a model. The testing results in this paper are significant for developing 5G mmW terrestrial links.

References

[1] YUAN Y F, ZHAO X W. 5G: vision, scenarios and enabling technologies [J]. ZTE communications, 2015, 13(1): 3 – 10. DOI: 10.3969/j.issn.1673.5188.2015.01.001
[2] MARCHETTI N. Towards 5th generation wireless communication systems [J]. ZTE communications, 2015, 13(1): 11–19. DOI: 10.3969/j.issn.1673.5188.2015.01.002
[3] LUO F L. Signal processing techniques for 5G: an overview [J]. ZTE communications, 2015, 13(1): 20 – 27. DOI: 10.3969/j.issn.1673.5188.2015.01.003
[4] HAN S F, I C-L and XU Z K. Energy-efficient large-scale antenna systems with hybrid digital-analog beamforming structure [J]. ZTE communications, 2015, 13(1): 28–34. DOI: 10.3969/j.issn.1673.5188.2015.01.004
[5] WONG V W.S, SCHOBER R. Key technologies for 5G wireless systems [M]. Cambridge, England: Cambridge University Press, 2017: 15 – 64
[6] MACCARTNEY G R, RAPPAPORT T S, SAMIMI M K, et al. Millimeter-wave omnidirectional path loss data for small cell 5G channel modeling [J]. IEEE access, 2015, 3: 1573–1580. DOI: 10.1109/access.2015.2465848
[7] SAMIMI M K, RAPPAPORT T S. 3-D millimeter-wave statistical channel model for 5G wireless system design [J]. IEEE transactions on microwave theory and techniques, 2016, 64(7): 2207–2225. DOI: 10.1109/tmtt.2016.2574851
[8] MACCARTNEY G R, RAPPAPORT T S, SUN S, et al. Indoor office wideband millimeter-wave propagation measurements and channel models at 28 and 73 GHz for ultra-dense 5G wireless networks [J]. IEEE access, 2015, 3: 2388–2424. DOI: 10.1109/access.2015.2486778
[9] ISHIMARU A. Electromagnetic wave propagation, radiation, and scattering [M]. Hoboken, USA: John Wiley & Sons, 2017. DOI: 10.1002/9781119079699
[10] GONG S H, GAO Y F, SHI H B, et al. A practical MGA-ARIMA model for forecasting real-time dynamic rain-induced attenuation [J]. Radio science, 2013, 48(3): 208–225. DOI: 10.1002/rds.20028
[11] GONG S H, WEI D X, XUE X W, et al. Study on the channel model and BER performance of single-polarization satellite-earth MIMO communication systems at Ka band [J]. IEEE transactions on antennas and propagation, 2014, 62 (10): 5282–5297. DOI: 10.1109/tap.2014.2342754
[12] XU X L, LIU M, XIONG J B, et al. Key technology and application of millimeter wave communications for 5G: a survey [J]. Cluster computing, 2019, 22(S5): 12997–13009. DOI: 10.1007/s10586-018-1831-x
[13] NIU Y, LI Y, JIN D P, et al. A survey of millimeter wave communications (mmwave) for 5G: opportunities and challenges [J]. Wireless networks, 2015, 21(8): 2657–2676. DOI: 10.1007/s11276-015-0942-z
[14] ICHKOV A, ATANASOVSKI V, GAVRILOVSKA L. Potentials for application of millimeter wave communications in cellular networks [J]. Wireless personal communications, 2017, 92(1): 279–295. DOI: 10.1007/s11277-016-3850-3
[15] ZHOU L, XIAO L M, YANG Z, et al. Path loss model based on cluster at 28 GHz in the indoor and outdoor environments [J]. Science china information sciences, 2017, 60(8): 080302. DOI: 10.1007/s11432-017-9127-6
[16] JAECKEL S, RASCHKOWSKI L, WU S B, et al. An explicit ground reflection model for mm-wave channels [C]//IEEE Wireless Communications and Networking Conference Workshops (WCNCW). San Francisco, USA: IEEE, 2017: 19–22. DOI: 10.1109/wcncw.2017.7919093
[17] RAPPAPORT T S, SUN S, SHAFI M. 5G Channel model with improved accuracy and efficiency in mmwave bands [J]. IEEE 5G tech focus, 2017, 1(1): 1–6
[18] ZHAO X W, LI S, WANG Q, et al. Channel measurements, modeling, simulation and validation at 32 GHz in outdoor microcells for 5G radio systems [J]. IEEE access, 2017, 5: 1062–1072. DOI: 10.1109/access.2017.2650261
[19] RAPPAPORT T S, SUN S, SHAFI M. Investigation and comparison of 3GPP and NYUSIM channel models for 5G wireless communications [C]//IEEE 86th Vehicular Technology Conference (VTC-Fall). Toronto, Canada: IEEE, 2017: 24–27. DOI: 10.1109/vtcfall.2017.8287877
[20] ZHANG X, ZHAO Z W, LIN L K, et al. Rain attenuation characterization on 5G millimeter wave links with short distance [J]. Chinese journal of radio science, 2017, 32(5): 507–512, 2017.DOI: 10.13443 / j.cjors.2017091901
[21] GARCIA-RUBIA J M, RIERA J M, BENARROCH A, et al. Estimation of rain attenuation from experimental drop size distributions [J]. IEEE antennas and wireless propagation letters, 2011, 10: 839 – 842. DOI: 10.1109/lawp.2011.2163609
[22] BLEVIS B. Losses due to rain on radomes and antenna reflecting surfaces [J]. IEEE transactions on antennas and propagation, 1965, 13(1): 175–176. DOI: 10.1109/tap.1965.1138384
[23] KHARADLY M M Z, ROSS R. Effect of wet antenna attenuation on propagation data statistics [J]. IEEE transactions on antennas and propagation, 2001, 49(8): 1183–1191. DOI: 10.1109/8.943313
[24] GONG S H, HUANG J Y, ZHAO X L. Rain-induced effects on the envelope probability density functions in multipath channels [J]. Radio science, 2008, 43(2): 1–11. DOI: 10.1029/2007rs003759

Biographies

GONG Shuhong (shgong@xidian.edu.cn) received the M.S. and Ph.D. degrees in radio physics from Xidian University, China in 2004 and 2008, respectively. Now, he is a professor and a doctorial tutor at Xidian University. His research interest focuses on radio wave propagation in near-earth space and its applications.

ZHANG Xingmin is currently working toward the M.S. degree in radio physics from Xidian University, China. His current research interest is MIMO wireless channel modeling for 5G communication system.

DOU Jianwu received the Ph.D. degree from Beijing University of Technology, China in 2001. Since 2001, he has been in charge of research and system design of the radio resource management algorithm in UMTS, TD-SCDMA and LTEv1 at ZTE Corporation. From 2006, he has also been responsible for system simulation of 2G, 3G, 4G, and WLAN as a department director at ZTE Corporation. His research interests include RRM, system simulation, wireless channel sounding and modelling, data mining, high frequency physical layer design, and MTC.

HUANG Weifang received the master degree in electromagnetic field and microwave technology from the School of Electronic Engineering, Xidian University, China in 2006. He is a senior engineer of the Algorithm Department, ZTE Corporation. Since May 2008, he has been engaged in the research of the communication system. His main research directions are wireless environment modeling, high-frequency communications, and communication system networking simulation modeling.